Chapter 8

Scour Caused by Wall Jets

Ram Balachandar and H. Prashanth Reddy

Additional information is available at the end of the chapter

http://dx.doi.org/10.5772/54909

1. Introduction

Scour that results directly from the impact of the hydraulic structure on the flow and which occurs in the immediate vicinity of the structure is commonly called local scour. It is very important to reduce local scour caused by impacting jets. A thorough understanding of the erosion of the bed due to local scour remains a challenge since it is associated with a highly turbulent flow field. The size, shape and density of sand particles, flow velocity, flow depth, turbulent intensity and shape of scour hole influence the complex processes of entrainment, suspension, transportation and deposition of sediment. This chapter briefly discusses transport and local scour mechanism of cohesionless sand caused by plane, two-dimensional and three-dimensional wall jets. The aim of the chapter is to facilitate the reader to understand scour characteristics, scour profile measurements, effects of tailwater depth, sand grain size, width of the channel, laboratory test startup conditions and scour that occurs under ice cover conditions.

2. Scour hole characteristics

The scour hole formation by various forms of jets (e.g., circular, two-dimensional (2D) and three-dimensional (3D)) can destabilize a hydraulic structure in the immediate vicinity of the jet. A typical visual example of the scour process caused by a 2D jet is presented herein to illustrate the complexity of the flow. As the flow is commenced, the jet exits the nozzle or the sluice gate, interacts with the bed and scouring action takes place. This is usually called the digging phase. During digging, the jet is directed towards the bed, a hole is formed and the excavated sand is deposited as a mound just downstream of the scour hole. The scouring process is very rapid in this phase. The location of the impingement point changes in the longitudinal direction during the digging process. Following the digging period, the jet flips towards the free surface and a refilling process is commenced. In this phase, the water surface

tends to be wavy. The surface jet impinges on the mound region and some of the sediment deposited on the mound falls back and refills the scour hole. In time, the jet suddenly flips back towards the bed and once again causes rapid digging of the bed with lifting of the bed material into suspension. The free surface is not wavy during the rapid digging process. An intermediate hump is formed in the scour hole. In time, the jet is once again directed towards the free surface and refilling occurs. The alternate digging and refilling occurs only at low tailwater depths. The asymptotic condition (i.e., when changes to the bed profile is minimal) is attained after a very long time period. The above process is illustrated in Fig. 1 (Balachandar et al. 2000). Fig. 1(a) shows the end of a refilling cycle prior to the commencement of the digging process. Fig. 1(b) shows the beginning of digging phase, with a recirculating flow region rotating in a clockwise direction being formed upstream of impingement and a counter clockwise roller formed in the downstream section. Fig. 1(c) shows sand is primarily transported by advection of suspended particles. Fig. 1(d) shows a relatively calm water surface profile during the digging phase. The redirection of the jet towards the water surface (surface jet) after the end of digging phase causes the water surface to become wavy (Figs. 1e, 1f and 1g). Refilling takes place in Figs. 1(f) and 1(g). Fig. 1(h) shows the reoccurrence of digging phase. Studying the effects of tailwater depth, flow properties and sediment properties on the scour hole dimensions will help in better predicting the scour hole geometry.

The definition sketch of the scour hole geometry is shown in Fig. 2 (Sui et al. 2008). Several researchers including Dey and Sarkar (2006a, b), Pagliara et al. (2006) and Balachandar et al. (2000) studied the role of the following geometrical and hydraulic parameters governing the scour process:

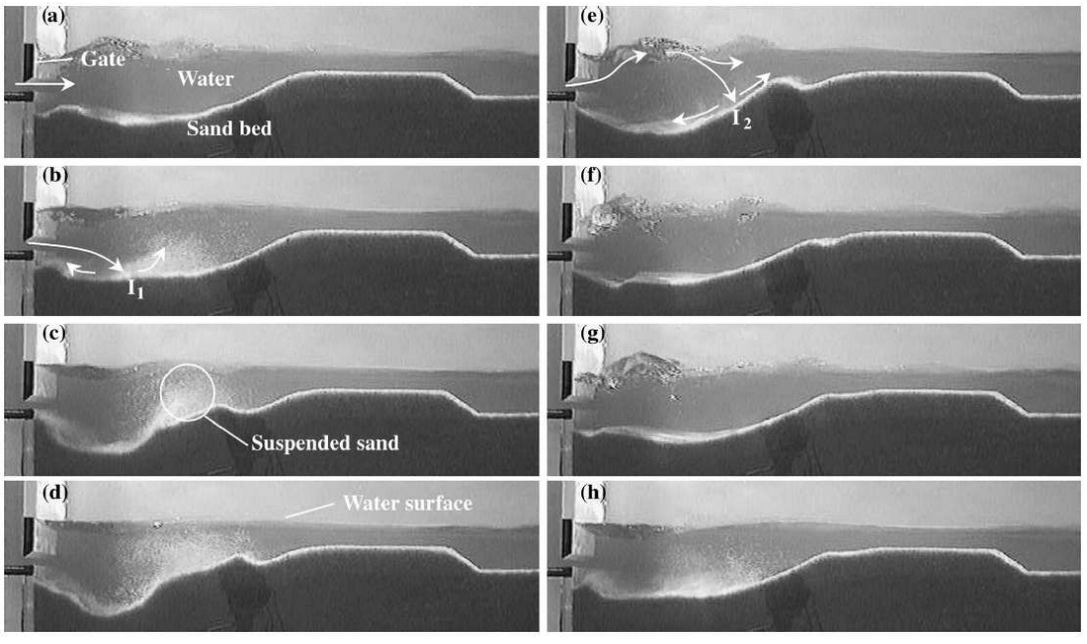

Figure 1. Demonstration of local scour cycle: (a) scour begins; (b) digging phase commences; (c) digging continues; (d) maximum digging; (e) filling phase begins; (g) maximum fill; (h) reoccurrence of digging phase. (Balachandar et al. 2000, copyright permission, NRC Research Press)

http://dx.doi.org/10.5772/54909

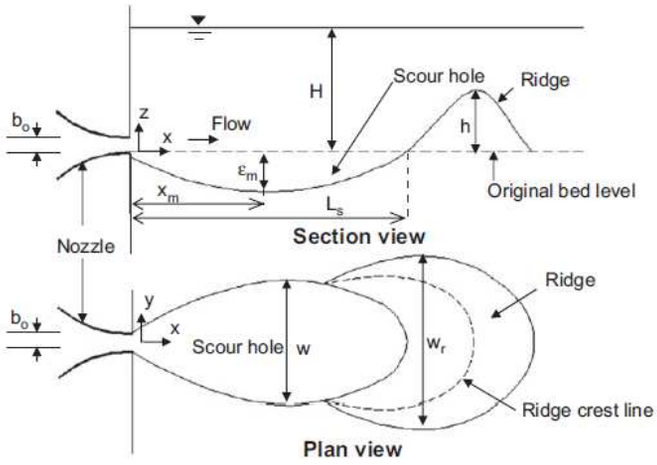

Figure 2. Definition of scour parameters (Sui et al. 2008, copyright permission of Science Direct)

i. Nozzle hydraulic radius (defined as $b_o/4$)

ii. Jet exit velocity (U_o) - the undiminished mean velocity in potential core

iii. Grain size - generally, the median grain size (d_{50}) of the cohesionless bed is considered as the representative grain size

iv. Densimetric Froude number (F_o) -$F_o = U_o / \sqrt{g d_{50} \Delta\rho / \rho}$, $\Delta\rho$is submerged density of bed material, and ρ is density of bed material.

v. Tailwater depth (H or y_t) - defined as depth of water over the original bed

vi. Channel width (W) - the width of downstream channel into which the jet is exiting

vii. Expansion ratio (ER) - channel width to jet thickness,

viii. Time evaluated from the start of the flow (t)

ix. Submergence ratio - tailwater depth to the thickness of the jet at its origin.

The variables of interest include:

i. Maximum scour depth (ε_m)

ii. Location of maximum scour depth (x_m or δ) from the nozzle exit

iii. Volume of scour (V) - measured by determining volume of the water needed to fill the scour hole.

iv. Scour hole length (L_s) - maximum extension of the scour hole along the midsection.

v. Scour hole width (w)- maximum extension of the scour hole measured perpendicular to the flow direction.

vi. Ratio of the length of the scour hole at asymptotic conditions to jet exit velocity (L_s / U_o)

Rajaratnam and Berry (1977), Lim (1995), Aderibigbe and Rajaratnam (1996), Ade and Rajaratnam (1998) and Sui et al. (2008) studied wall jet scour and concluded that the key parameter that effects the scour hole dimensions is F_o. Sediment uniformity also influences the scour geometry. The formation of the armor layer in non-uniform beds leads to smaller scour geometry when compared to that formed in uniformly distributed sediment (Aderibigbe and Rajaratnam 1996, Mih and Kabir 1983). In general, it has been assumed that the effect of the sediment size on scour hole dimensions can be absorbed by the densimetric Froude number (Rajaratnam (1981), Mazurek and Rajaratnam (2002) and Rajaratnam and Mazurek (2003)). The influences of the various factors are described in the forthcoming sections. Sui et al. (2008) investigated the effect of the sediment size on scour hole dimensions in detail.

The effect of tailwater depth on the scour hole dimensions due to impinging and free falling jets have been investigated by Ghodsian et al. (2006) and Aderibigbe and Rajaratnam (1996). Critical values of the tailwater depth were introduced by Aderibigbe and Rajaratnam (1996) and Ghodsian et al. (2006) such that beyond the critical value (either by increasing or decreasing the tailwater depth), the scour hole dimensions decreased. However, Ali and Lim (1986), Faruque (2004), Sarathi et al. (2008) and Mehraein et al. (2010) have stated that scour hole dimensions due to 2D and 3D wall jets increase either by increasing or decreasing the tailwater depth from the critical value.

3. Scour due to wall jets

3.1. Characteristics of two–dimensional wall jets

Mohamed and McCorquodale (1992) investigated the local scour downstream of a rectangular opening with a swept-out hydraulic jump and identified two stages of local scour development.

i. An initial stage of local scour which occurs rapidly (short-term scour).

ii. A progressive stage which approaches equilibrium after a very long time (long-term scour).

Mohamed and McCorquodale (1992) observed that the equilibrium depth for short-term scour established rapidly in less than 1% of the time to reach the long-term scour depth. The short-term scour although not as deep as the long-term scour occurs much closer to the apron; the bed is more highly fluidized than in the regime that governs the long-term scour. They have also stated that short-term scour due to plane horizontal supercritical jets under low tailwater conditions is related to the energy dissipation regime that dominates the flow. They identified seven different jet forms:

1. Attached jet: Bottom boundary of jet conforms to the bed and top boundary of jet forms the free surface from beginning of jet exit.

2. Moving jump: Hydraulic jump formed by the jet is propagating downstream.
3. Wave jump: Standing wave type of hydraulic jump is formed downstream of the jet exit.
4. Surface jet: Top boundary of jet forms the free surface and bottom boundary of jet is not confined.
5. Plunging jump: Jet is plunging down along the slope of the scour hole. Specifically, the bottom boundary is along the slope of scour hole and top boundary of jet is submerged.
6. Inverted jump: Top and bottom boundaries of jet try to attain the free surface and bed, respectively, beyond scour hole.
7. Classical jump (as in stilling basins)

The more rapid short-term scour was associated with regimes 1, 2, 3 and 6, while the deeper long-term scour was associated with regimes 4 and 5 indicated above.

Rajaratnam (1981) found that maximum depth and length of scour hole increased linearly with the logarithm of time. He noted that the scour hole reached an asymptotic stage. Rajaratnam (1981) concluded that maximum depth and length of scour are largely dependent on the densimetric Froude number. Johnston (1990) investigated three different scour hole regimes created in shallow tailwater conditions. Two scour hole regimes were formed when the jet permanently attaches itself to either the bed or free surface boundary whilst the third was formed when the jet periodically flips between the free surface and channel bed. Johnston (1990) found that the scour hole development in deep water conditions is orderly and invariably reaches a well-defined asymptotic state while in shallow conditions such a state is sometimes not reached. The depth of flow has a considerable influence on the near bed flow field and may promote the flipping of the jet from one boundary to another. Balachandar et al. (2000) suggested that tailwater depth was a key parameter when tailwater depth was less than 16 times the nozzle thickness or sluice gate opening (b_o). Chatterjee et al. (1994) found that maximum scour depth is a function of Froude number based on nozzle thickness ($F = U_o / \sqrt{g b_o}$). Kells et al. (2001) concluded that scour geometry is dependent on sediment bed grain size and initial jet exit velocity (U_o). Ali and Lim (1986) have developed the following power law relationship for time evolution of scour:

$$\frac{V}{R^3} = 187.72\left(\frac{\varepsilon_m}{R}\right)^{2.28}$$

where, V is the volume of scour and R is hydraulic radius and ε_m is maximum scour depth.

3.2. Scour characteristics of three–dimensional wall jets

Scour caused by 3D and circular wall jets have been studied by Meulen and Vinje (1975), but to a lesser degree than that caused by plane and impinging jets. Rajaratnam and Berry (1977) studied the scour caused by circular wall jets on cohesionless soils. They concluded that the geometric characteristics of the scour hole mainly depend on the densimetric Froude number. Rajaratnam and Berry (1977) also found that the jet expands in an unconfined manner from

the nozzle exit to the point of maximum scour depth. Ali and Lim (1986) concluded that for 3D jets, mean flow velocity for any section decreases continuously in the flow direction, whereas for two-dimensional flows, the mean velocity increases as the flow develops. In three-dimensional jet scour, no reverse flow was observed near the bed. It was observed in 3D flows that there were occasional turbulent bursts near the bed which moved sand particles from the upstream slope of the hole to the region of maximum scour. Ali and Lim (1986) have suggested the following power law relationship for time evolution of volume of scour:

$$\frac{V}{R^3} = 49.36\left(\frac{\varepsilon_m}{R}\right)^{1.89}$$

Hoffmans and Pilarczyk (1995) developed a semi-empirical relation for the upstream scour slope and verified the equation using experimental results. Lim (1995) studied the effect of channel width (expansion ratio) on scour development of 3D jets and concluded that there was no effect of channel width on scour development for expansion ratios greater than 10. The width of scour hole was affected by the width of downstream channel only when normal diffusion of the 3D jet flow is restricted in transverse direction. Rajaratnam and Diebel (1981) found that relative tailwater depth and relative width of downstream channel affect the location of maximum scour depth. Chiew and Lim (1996) developed the following empirical equations by using the densimetric Froude number (F_o) as the main characteristic parameter to estimate scour dimensions caused by circular wall jet:

$$\frac{\varepsilon_m}{b_o} = 0.21F_o \quad \frac{w}{b_o} = 1.90F_o^{0.75} \quad \frac{L}{b_o} = 4.41F_o^{0.75}$$

Ade and Rajaratnam (1998) further emphasized the use of F_o as the main parameter to analyze scour caused by circular wall jets. However, they noted that asymptotic dimensions of scour hole are dependent on tailwater depth for $F_o > 10$. Ade and Rajaratnam (1998) also found that the eroded bed profile near the nozzle attains asymptotic state earlier than locations away from nozzle.

4. Role of fluid structures on two–dimensional scour

Hogg et al. (1997) have pointed out that a comprehensive understanding of the scour remains elusive because of the complex nature of the flow field. Rajaratnam (1981), Rajaratnam and Macdougall (1983), Wu and Rajaratnam (1995) and Rajaratnam et al. (1995) have made significant contributions despite the complexity resulting from the hydrodynamic characteristics of the jet and the concave shape of eroded bed. Hopfinger et al. (2004) proposed new scaling laws relating time and the attainment of the quasi-steady scour depth. They suggested that turbulence created by Gortler vortices cause sediment transport and the associated scouring mechanism due to the destabilization of the turbulent wall layer by the concave curvature of the water sediment interface. Bey et al. (2007) studied the velocity field during asymptotic conditions in the scoured region to understand the role of turbulent flow structures that influence scour and evaluated higher-order velocity moments. Experimental findings of Bey et al. (2007) are presented here.

http://dx.doi.org/10.5772/54909

Bey et al. (2007) carried out two tests at exit velocities of 1.0 m/s and 1.27 m/s (Tests A and B) and at a tailwater depth (H) corresponding to 20 b_o continuously for 12 days duration. These tests can be classified under the high submergence flow regime. The high and low submergence is not clearly defined in literature, however high submergence can be defined as a state where no alternate flicking of the jet between the free surface and bed occurs as in low submergence cases (Balachandar et al. 2000). Generally, a value of $H/b_o > 10$ has been considered as high submergence. The time to reach asymptotic conditions was found to be as low as t = 24h depending on scour hole and ridge geometric parameter chosen. For example, the total length of the scour affected region (L_T) attains an asymptotic state at t = 24h, however the change in the maximum depth of the scour hole (ε_m) is less than 5% after t = 48h. However, it should be noted that beyond 72h, there is the presence of the turbulent bursts which cause local changes in the location of the maximum depth of scour profile (x_m) but no significant changes in the mean scour profile. Sectional and plan view of the scour region along with the definition of various variables are shown in Fig. 3(a).

Bey et al. (2007) divided the entire test duration from the start of flow to the attainment of asymptotic conditions into five time zones to study the influence of the different flow structures. A time scale $T = L_s/U_o$ is used to non-dimensionalize the five time zones, where L_s is length of scour hole at asymptotic conditions. Fig 3(b) shows variation of important scour parameters with time in five time zones. Each of the time zones had certain dominant flow features. Flow was characterized by the presence of longitudinal vortices and turbulent bursts at the start of the test and during early time periods, and movement of the jet impingement point during the later stages. Scour was very rigorous during first time zone ($t/T \leq 850$). A 2D hole was formed downstream of the nozzle and the bigger size particles were deposited further downstream as a 2D mound. In second time zone ($850 \leq t/T \leq 15\text{x}10^3$), the large-scale suspension of the bed material seen in the earlier time zone was reduced significantly. No major scour happened in the negative slope region (Fig. 3a). Two or three longitudinal streaks and very prominent concave depressions were observed. Hopfinger et al. (2004) reported that vortices due to Gortler instability caused scour on the positive bed slope. During the third time zone ($15\text{x}10^3 \leq t/T \leq 125\text{x}10^3$), there appeared a "scoop-and-throw" like scouring action on either side of the flume axis, which caused longitudinal concave shaped depressions. A lifting spiraling motion of bed particles occurred near the end of concave shaped depression due to vortex activity. Dye injection confirmed the presence of spiral motions during the fourth time zone ($125\text{x}10^3 \leq t/T \leq 375\text{x}10^3$) and also scoop-and-throw like scouring action slowed down after 24 h. The scour hole attained an asymptotic state in the fifth time zone after 72 hours of scour process ($t/T \geq 375\text{x}10^3$). In the asymptotic stage, turbulent bursts were noticed to occur in the near bed region across the section of the flume. In addition, two prominent scour mechanisms occurred on either side of the flume axis causing the bed particles to be spiraled toward the sidewalls from midsection and from sidewalls to the flume axis. However, no particle movement was observed along the nozzle axis.

At asymptotic conditions, scour profile in the scour hole region was nominally two-dimensional across the width of the flume. It should be remarked that the backward and forward move-

ment of the jet contact point with bed, the frequent but random turbulent bursts, and the two prominent scour mechanisms (digging and refilling), all occurred at one time or the other. However, in the mound region, the lateral profile was not two-dimensional and had two distinct peaks. These peaks occurred closer to the sidewalls leaving a trough in center portion of the mound. Jet impingement point on the bed moved backward and forward, and the mean location of point of contact of jet with bed was close to the deepest point of scour hole. Wide range of variation in instantaneous velocity from positive to negative values was a clear indication of back and forth movement of jet. It was observed that most of the turbulence activity occurred in the region of near-zero slope of scour hole. Analysis of third-order moments and quadrant decomposition indicated sweep type events in the near bed region contributed to scour. Ejection events near the bed caused suspension of the bed particles to be carried away by the average flow velocity. Measured velocities at asymptotic conditions were extrapolated to other time periods to conclude that the sweep and ejections contributed significantly to the scour process.

Figs. 4(a) and (b) show the flow fields for the tests A and B in the scour hole region at asymptotic conditions. Velocity vectors show that the jet expands vertically to interact with the bed. A large-scale recirculating region was found in the region above the jet axis, which extended to about $35b_o$ downstream of the jet. The center of this region was located at about $16b_o$ along the x-axis and about $10b_o$ along the y-axis. It is important to recognize that this recirculation region caused significant negative vertical velocities immediate vicinity of nozzle. Impact of the jet on the bed also generated a flow separation near the region close to the nozzle. A similar flow field was also observed in test B, which is qualitatively similar to that obtained in test A, and is shown in Fig. 4(b). The mean impingement point in test B occurs farther from the nozzle and consequently has a larger near-bed recirculation zone.

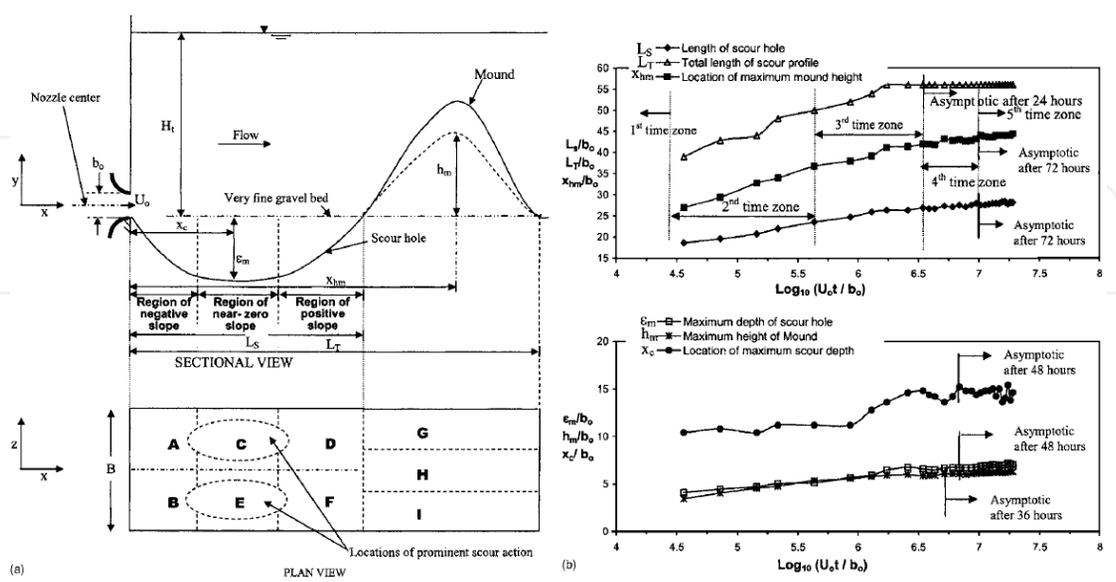

Figure 3. a) Definition sketch, (b) Variation of scour parameters with time (Bey et al. 2007, copyright permission of ASCE)

http://dx.doi.org/10.5772/54909

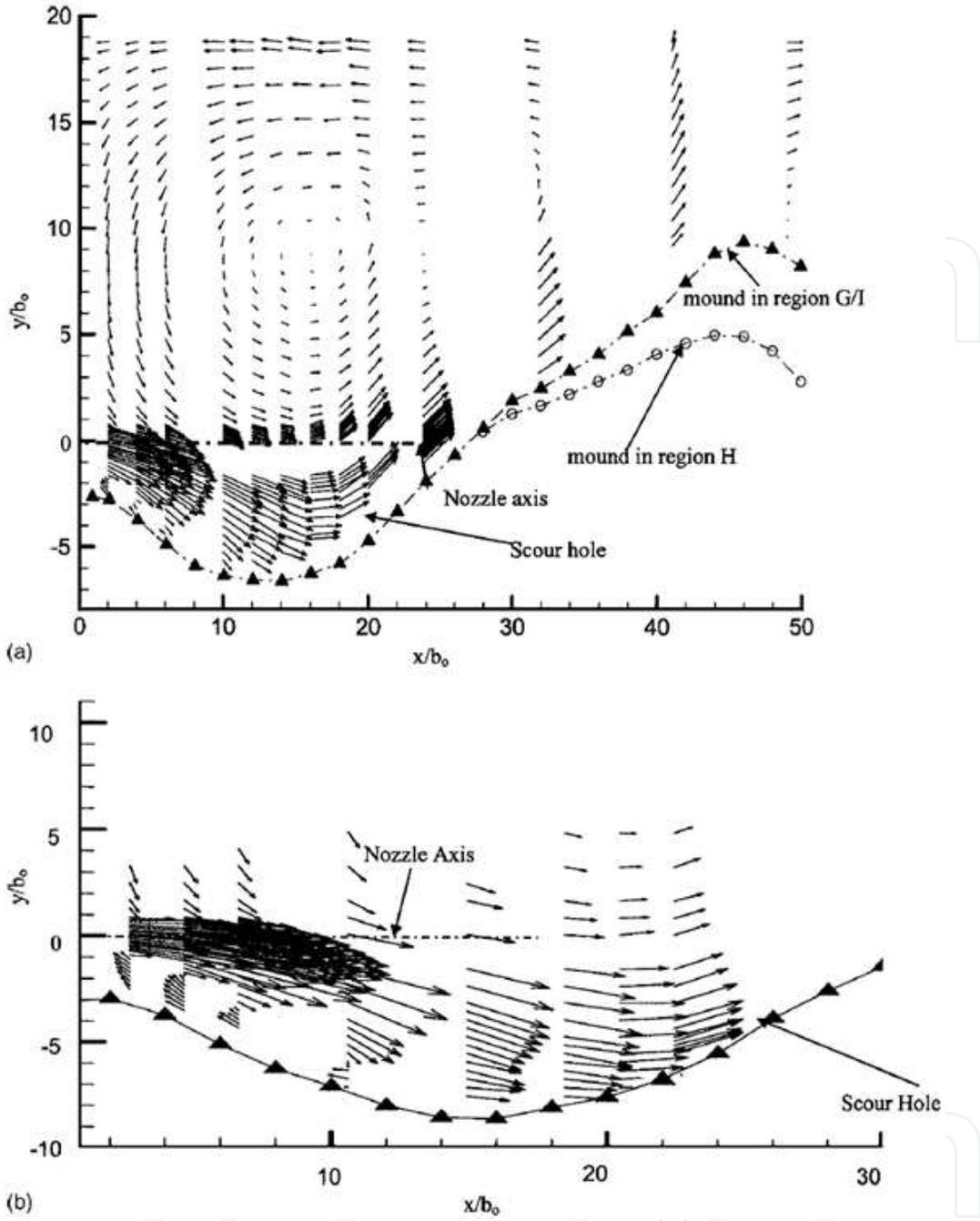

Figure 4. Velocity vector plot for (a) Test A; (b) Test B (Bey et al. 2007, copyright permission of ASCE)

5. Measurements using video image analysis

Figures 5(a) and 5(b) show a set of water surface profiles at about 840 seconds from the start of scour process. The profiles were obtained using a software called PROSCAN developed by Balachandar and Kells (1998). The time t_o refers to the start of the cycle. Figure 5(a) shows the

water surface profile during the digging phase and Fig 5(b) shows the water surface profiles during the refilling phase. Figure 5(c) shows bed scour profiles corresponding to the water surface profiles shown in Figs. 5(a) and 5(b). The bed profiles reflect the alternate digging and refilling phases as explained ealier. At $t = t_o$, the bed surface profile is similar to that provided by Rajaratnam (1981) where the water surface profiles are similar during digging and refilling phases. In the study of Balachandar and Kells (1998), the bed profile at $t = t_o$+2 s is quite different from initial bed profile at $t = t_o$. It is observed that at $t = t_o$ +2 s, the dynamic flow field indicates the digging phase near the sluice gate and piling up of sand (hump) on downstream side. After $t = t_o$ + 24 s, during the refilling phase, the sand particles in the hump part moved upstream and eventually refilled the trough. The refilling phase occurred over a longer period of time and the refilling process was nearing completion at $t = t_o$+179 s and profile eventually became similar to the profile shape recorded at $t = t_o$.

5.1. Computational stereoscopy

Ankamuthu et al. (1999) developed a stereoscopy scheme to measure the depth of scour in three-dimensional flow fields. The stereoscopy scheme makes use of an epipolar constraint and a relaxation technique to match corresponding points in two images. A correlation technique was developed to eliminate false matches. The depth of scour was calculated using the parallax between the matched points. However, the method is yet to be used to measure scour in a practical flow field.

6. The effect of tailwater depth on local channel scour

Ali and Lim (1986) studied scour caused by 3D wall jets at shallow tailwater conditions and noted that tailwater had an influence on the maximum depth of scour at asymptotic conditions. Tailwater depth which is under or above a critical condition causes an increase in maximum depth of scour (Ali and Lim, 1986). Further analysis of their data indicates that the critical value of tailwater depth increases with increasing densimetric Froude number. Ade and Rajaratnam (1988) stressed the use of F_o as the characteristic parameter to describe scour caused by circular wall jets and noted that the maximum depth of scour was found to be larger at high ratio of tailwater depth to nozzle width and higher values of F_o, which is consistent with the measurements of Ali and Lim (1986). However, they noted that the asymptotic dimensions of the scour hole were dependent on the tailwater conditions for only F_o >10. Rajaratnam and Diebel (1981) concluded that the relative tailwater depth and relative width of the downstream channel do not affect the maximum depth of scour, whereas the location of the maximum scour was affected.

Faruque et al. (2006) presented the results of clear water local scour generated by 3D wall jets in a non-cohesive sand bed at low tailwater depths. They indicated that extent of scour of 3D wall jets is collectively influenced by the densimetric Froude number, tailwater depth, and grain size-to-nozzle width ratio. Each parameter has a dominant influence compared to other parameters at different flow conditions. For F_o < 5, tailwater depth has no effect on the

http://dx.doi.org/10.5772/54909

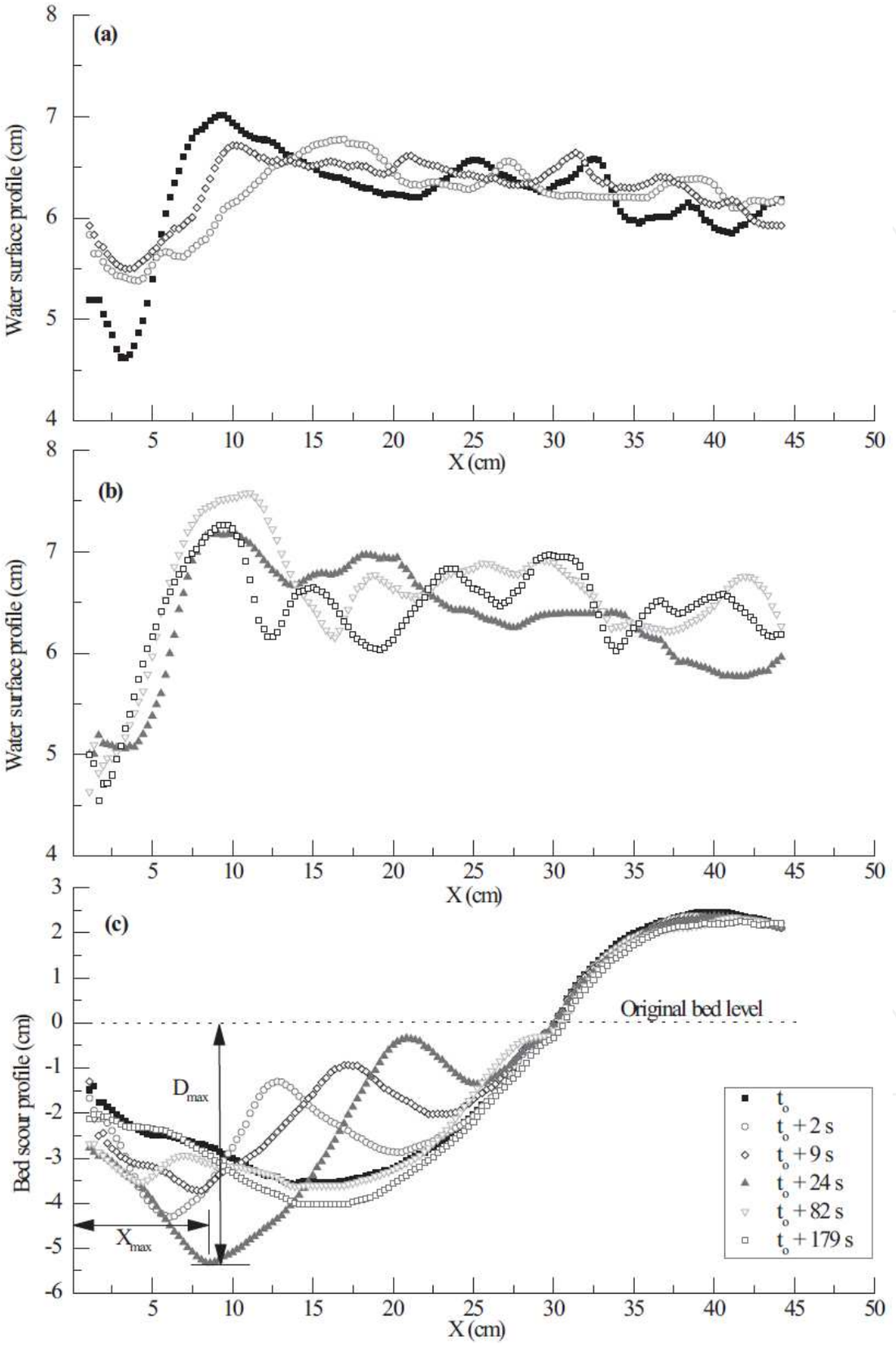

Figure 5. Variation of water surface profile and bed profile (after t = 823 s) (Balachandar and Kells, 1998, copyright permission of NRC Research Press)

maximum depth and width of scour. The effect of tailwater depth at higher densimetric Froude numbers appears to be important at larger values of non-dimensional sediment diameter (d_{50}/b_o). Previous observations have indicated that for $F_o > 10$, the effect of the tailwater depth was significant. However, the results of Faruque et al. (2006) clearly indicate that the effect of tailwater can be important at lower values of F_o depending on the value of d_{50}/b_o. At asymptotic conditions, comparing the volume of scour at $H/b_o = 6$ with that at $H/b_o = 4$, it was observed that the scour volume is greater at the higher tailwater depth. Faruque et al. (2006) also indicated that the maximum depth of scour is not necessarily deeper at higher values of tailwater depth in the lower range of submergences.

Experimental results of Faruque et al. (2006) are further discussed here. Three different tailwater depths (Tests A, B, and C) corresponding to $2b_o$, $4b_o$, and $6b_o$ where $b_o = 26.6$ mm and a jet exit velocity = 1.31 m/s (in the three tests) were considered in the experiments. The corresponding Reynolds number in the tests ($R_e = U_o b_o / \nu$) was 1.0 x 10^5 which shows prevalence of fully turbulent conditions. The flow Froude number based on exit velocity and nozzle width was 1.5, grain size was 0.85 mm and corresponding densimetric Froude number was six. Velocity measurements were obtained using a single component fibre-optic laser Doppler anemometer and scour profiles at different time intervals were obtained using a point gauge with an electronic display unit. Fig. 6(a) illustrates the time development of scour profiles along the nozzle axis for tests A, B and C. The profiles gradually attain an asymptotic state around $t = 48$ h. Fig. 6(a) also illustrates the maximum depth of scour (ε_m) and the location of maximum depth of scour from the nozzle exit (x_m) increase with increasing time. It was also found that the difference between two consecutive profiles at a fixed distance from the nozzle increases with increasing x. It should be noted that Ade and Rajaratnam (1988) found that maximum depth of scour to be larger at deeper submergences. In Figs. 6(b-d), the extent of scour is consistently larger at $H/b_o = 6$ at all t, and therefore the volume of scour at asymptotic conditions was greater for the larger submergence. The corresponding top view of the perimeter of the scour hole is shown in Figs. 7(a-e) which indicates that the perimeter of the sour hole is consistently larger at $H/b_o = 6$ as compared to $H/b_o = 4$. However, the hole perimeter expands laterally as depicted in Fig. 7(e) at $H/b_o = 4$ as asymptotic conditions are reached.

7. Effect of grain size on local channel scour

Scour occurs when the high velocity jet produces bed shear stresses that exceed the critical shear stress to initiate motion of the bed material. Critical shear stress of the bed material is a function of grain size and therefore, scour is a function of grain size. This section summarizes the effect of grain size on local scour. Breusers and Raudkivi (1991) discussed achievement of equilibrium state of scour and the similarity of scour profiles for various sizes of bed material and jet velocity. Balachandar and Kells (1997) studied the scour profile variation with time using a video imaging process on uniformly graded sediments caused by flow past a submerged sluice gate. Kells et al. (2001) investigated the effect of varying the grain size and, to a lesser extent, the grain size distribution of the erodible bed material on the scour characteristics. Figs. 8 and 9 are drawn from their study.

http://dx.doi.org/10.5772/54909

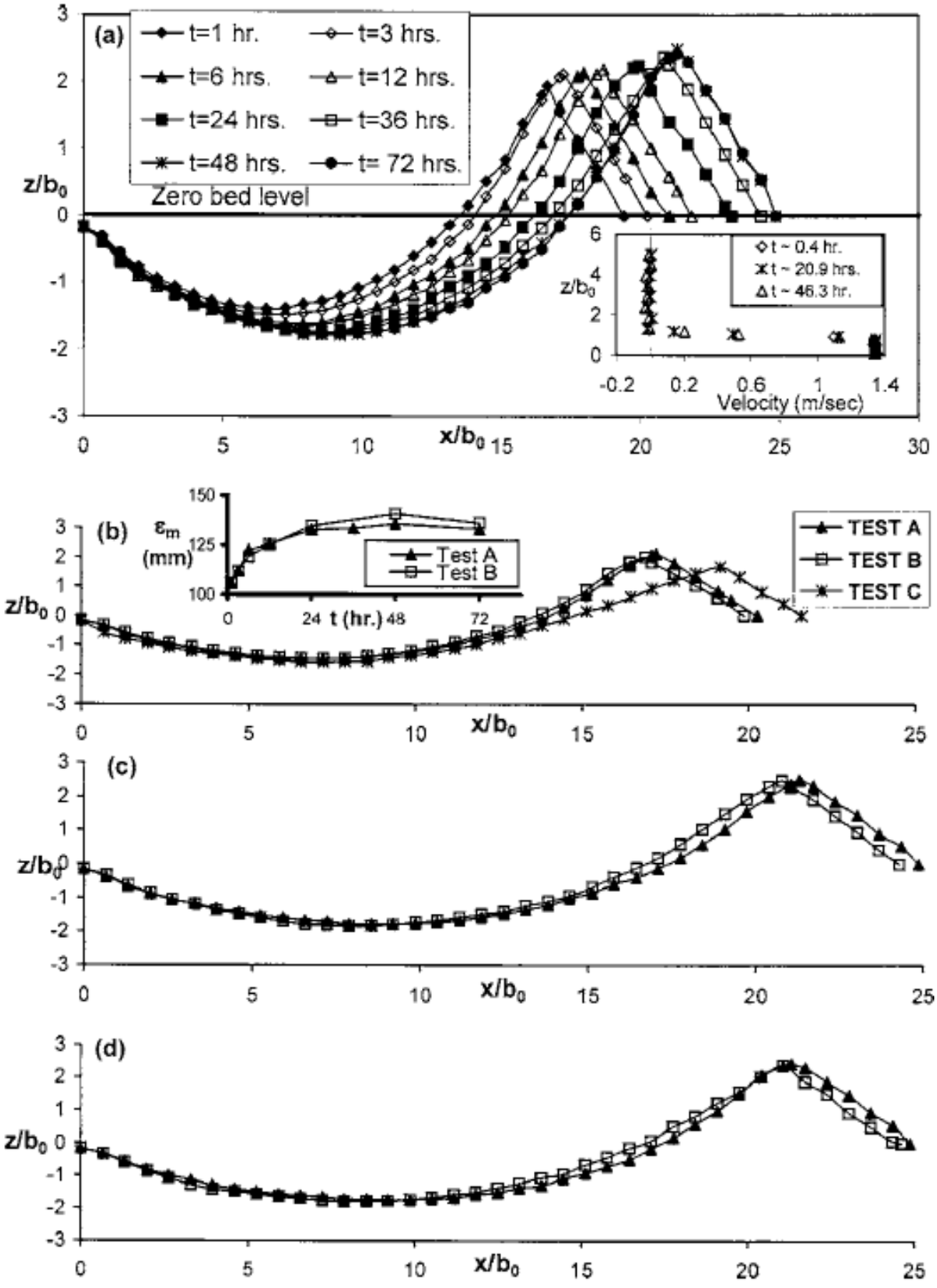

Figure 6. a) Development of scour profile along nozzle axis (b) comparison of scour profiles along nozzle centerline at $t = 3$ h; (c) $t = 48$ h; and (d) $t = 72$ h (Faruque et al. 2006, copyright permission of ASCE)

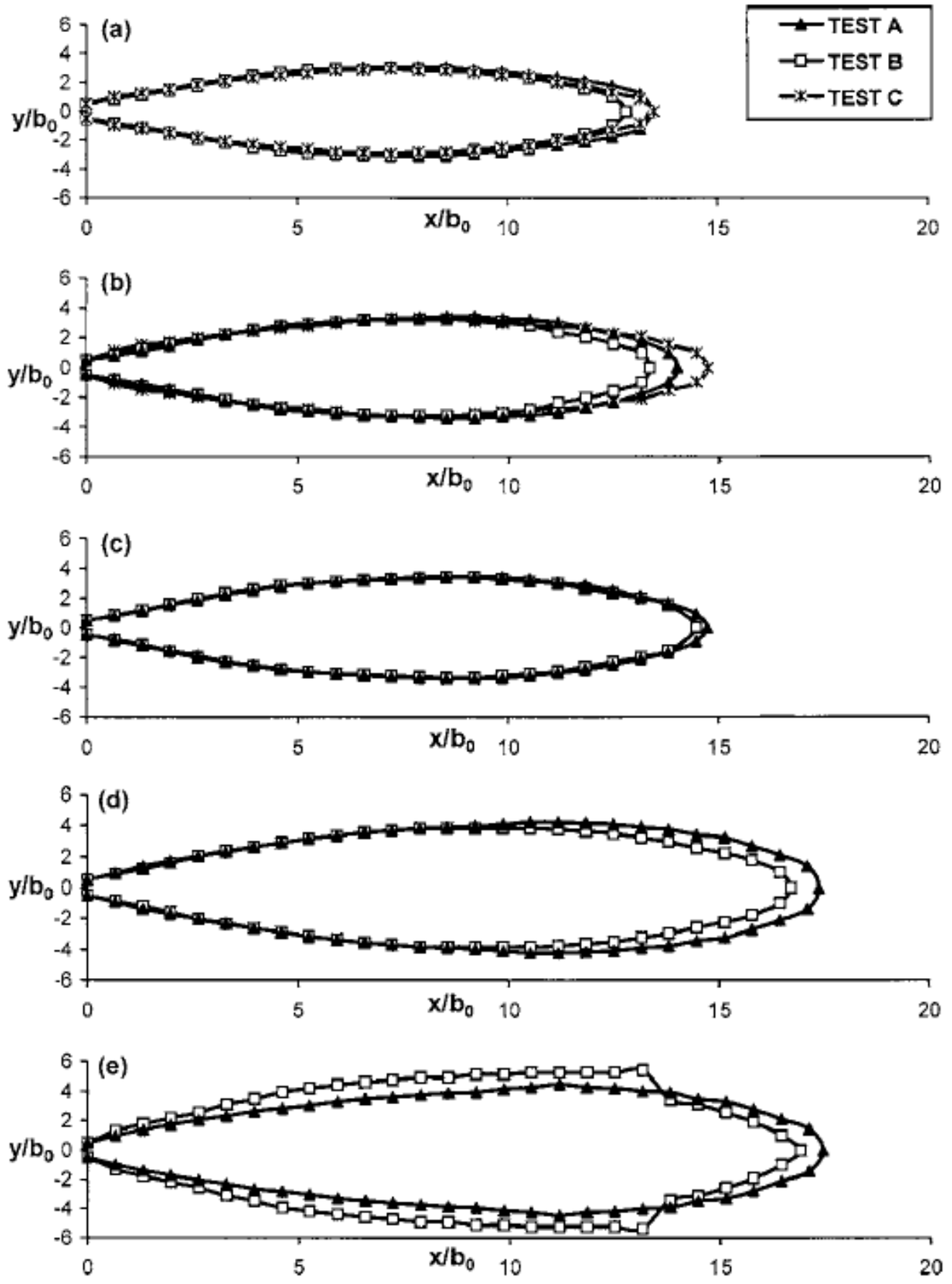

Figure 7. Comparison of plan view of perimeter of scour hole at various instances of time (a) t = 1 h; (b) t = 3 h; (c) t = 6 h; (d) t = 48 h; and (e) t = 72 h (Faruque et al. 2006, copyright permission of ASCE)

http://dx.doi.org/10.5772/54909

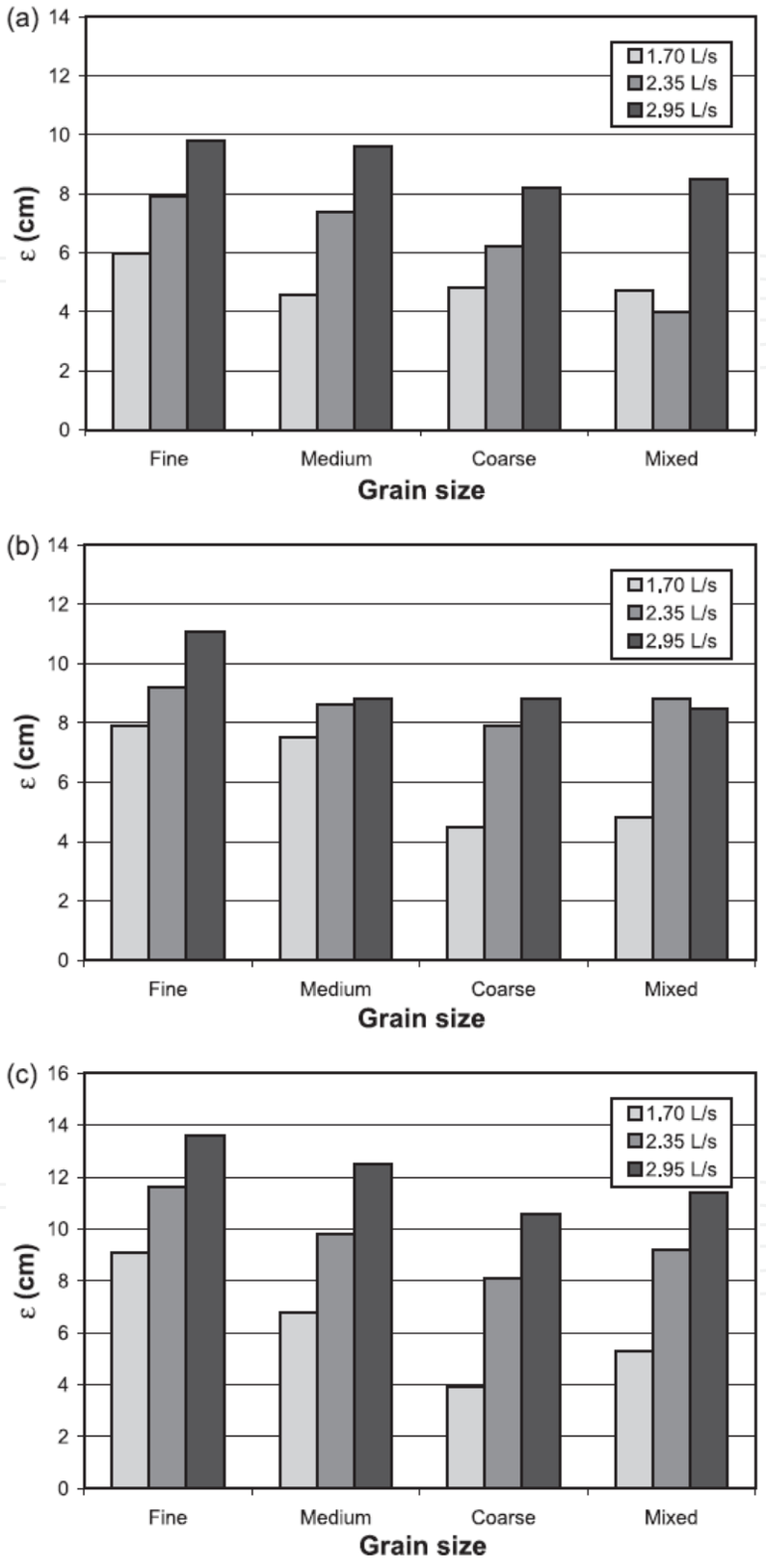

Figure 8. Effect of discharge and grain size on Phase-B maximum scour depth, ε_m, at t= 24h: (a) H/b_o = 4.0; (b) H/b_o = 6.3 and (c) H/b_o= 8.8 (Kells et al. 2001, copyright permission of NRC research press)

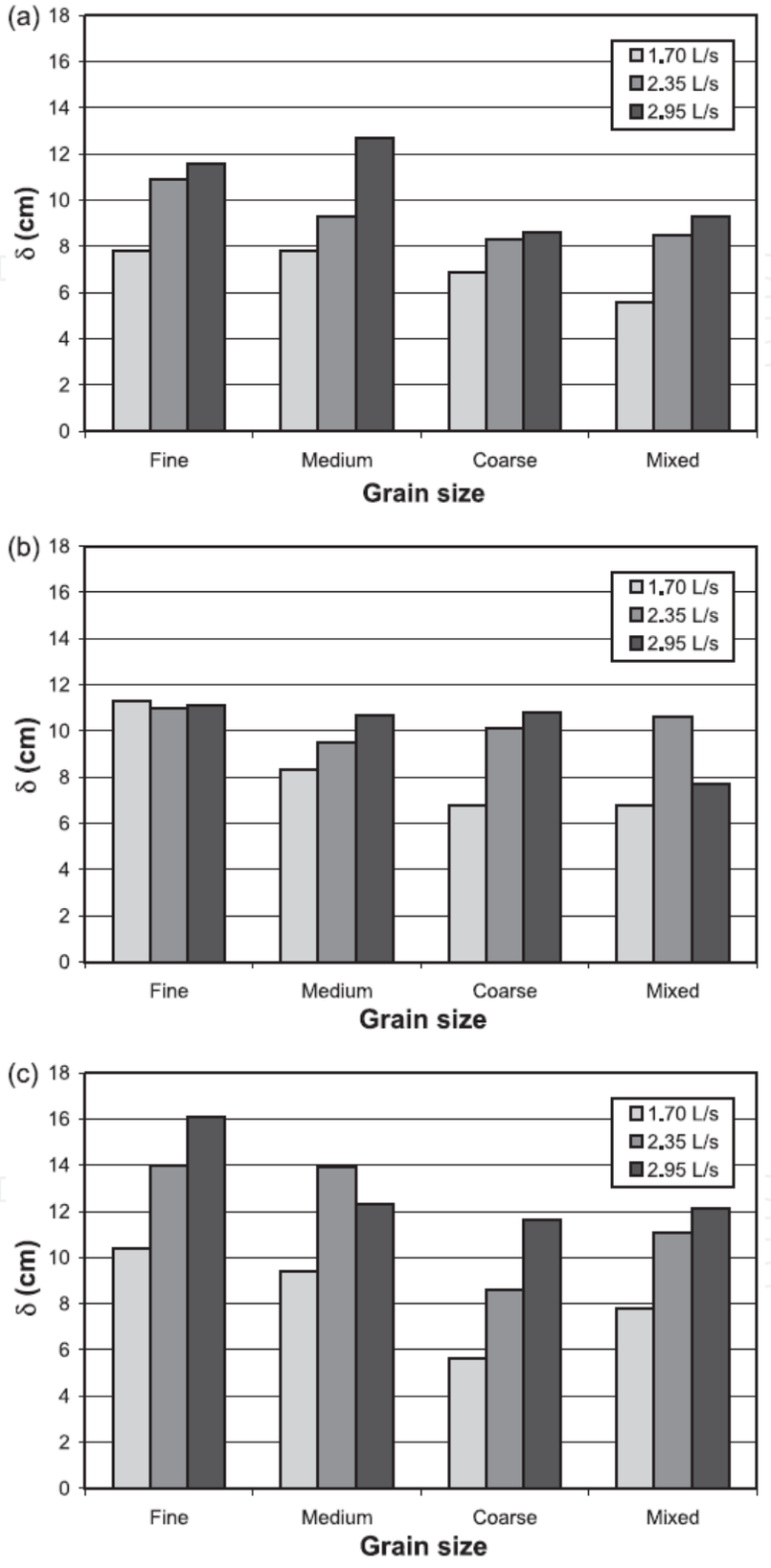

Figure 9. Effect of discharge and grain size on Phase-B location of point of maximum scour depth, x_m, at t= 24h: (a) H/b_o= 4.0; (b) H/b_o = 6.3 and (c) H/b_o= 8.8 (Kells et al. 2001, copyright permission of NRC research press)

http://dx.doi.org/10.5772/54909

The figures show the effect of grain size with increasing discharge and tailwater depth. Analysis of Figs. 8a, 8b, and 8c tell us that the magnitude of the maximum depth of scour (ε_m) increases with an increase in flow rate for a given grain size and maximum depth of scour decreases with increasing grain size for a given flow rate. It is also observed from Fig. 8 that maximum scour depth increases with increasing tailwater depth for a given grain size.

Figs. 9a, 9b, and 9c demonstrate that the location of maximum scour depth (δ) moves upstream with an increase in the grain size and moves downstream with increase in discharge. This is due to the fact that shear stress increases with increase in flowrate or critical shear stress decreases with decrease in grain size. The location of maximum scour depth (δ) moves downstream with increasing tailwater depth.

In summary, it was found that the grain size had a significant influence on the extent of scour, with more scour occurring with the smaller-sized material. Less scour occurred for graded sand (indicated as mixed sand in the figure) than a uniform one having a similar median grain size. Amount of scour increases with an increase in the discharge, hence the velocity of flow. For any given discharge and grain size, the greater the tailwater depth, the greater is the scour depth, extent, and volume of scour. It appears that the tailwater serves to slow the rate of jet expansion, thus increasing the length of bed exposed to high velocity, hence high shear stress conditions. It was also found that the tendency toward the dynamic alternating dig-fill cycling was lessened with a reduction in the discharge, or an increase in the grain size or the tailwater depth.

8. Effect of test startup conditions on local scour

A cursory evaluation of the test startup conditions in several of the studies mentioned in this chapter indicates that scour pattern is quite varied and depends on how the flow is initially commenced. For example, Kells et al. (2001) had the nozzle outlet plugged, whereas Balachandar et al. (2000) and Mohamed and McCorquodale (1992) had the sluice gate closed until proper head and tailwater conditions were established. Following this, the nozzle was unplugged or the sluice gate opened to a predetermined extent to generate the jet flow. This requires a certain amount of time before a steady jet discharge can be established. Rajaratnam (1981), Chatterjee et al. (1994), Mazurek (2002), and Aderibigbe and Rajaratnam (1998) created a suitable constant head difference between the downstream and upstream sections prior to generating the jet.

Johnston (1990) and Ali and Lim (1986) used a suitably sized aluminum sheet to cover the leveled bed in order to prevent it from being disrupted on commencement of the flow. The inflow was started; the flow and tailwater depths were then set to desired values, following which the sheet was slowly removed. It is thus clear that even for a seemingly simple flow emanating from nozzles or sluice gates, the flow and the corresponding scour pattern can become complex due to various influences and one among them is the startup condition.

Deshpande et al. (2007) investigated the effect of test startup conditions on plane turbulent wall jet behavior and the resulting scour profiles. The changing startup conditions also reflect

practical situations where the discharge and tailwater conditions change during regular operations. Deshpande et al. (2007) study also investigated the jet behavior and the different regimes of flow for a range of submergences (both low and high) using a laser Doppler anemometer (LDA). Furthermore, the effects of three different startup conditions on scour include an instantaneous startup condition, a gradual startup condition, and a stepwise startup condition were studied. Results of Deshpande et al (2007) are discussed below.

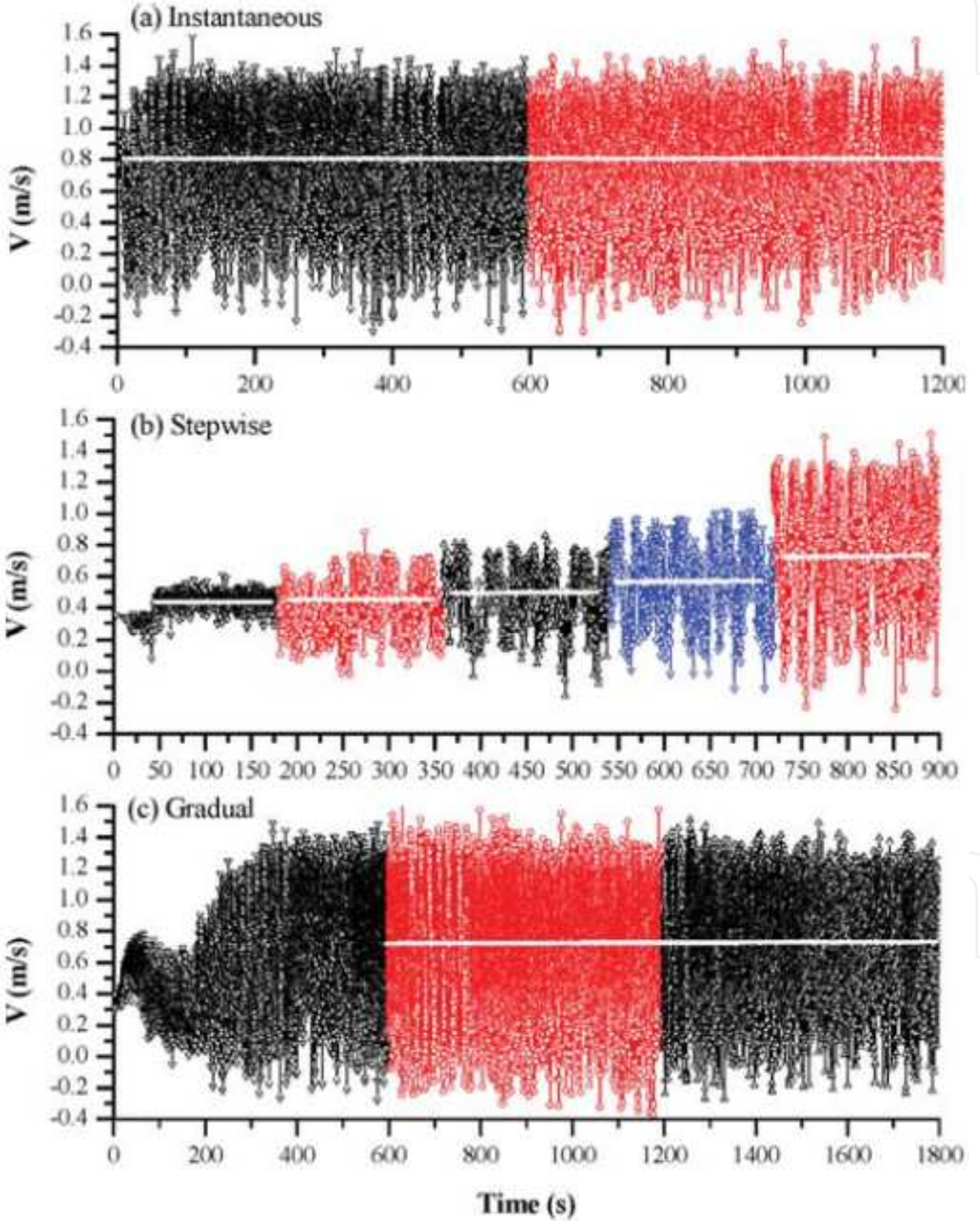

Figure 10. Effect of test startup conditions for H/b_o = 4 (Deshpande et al. 2007, copyright permission of Taylor and Francis)

http://dx.doi.org/10.5772/54909

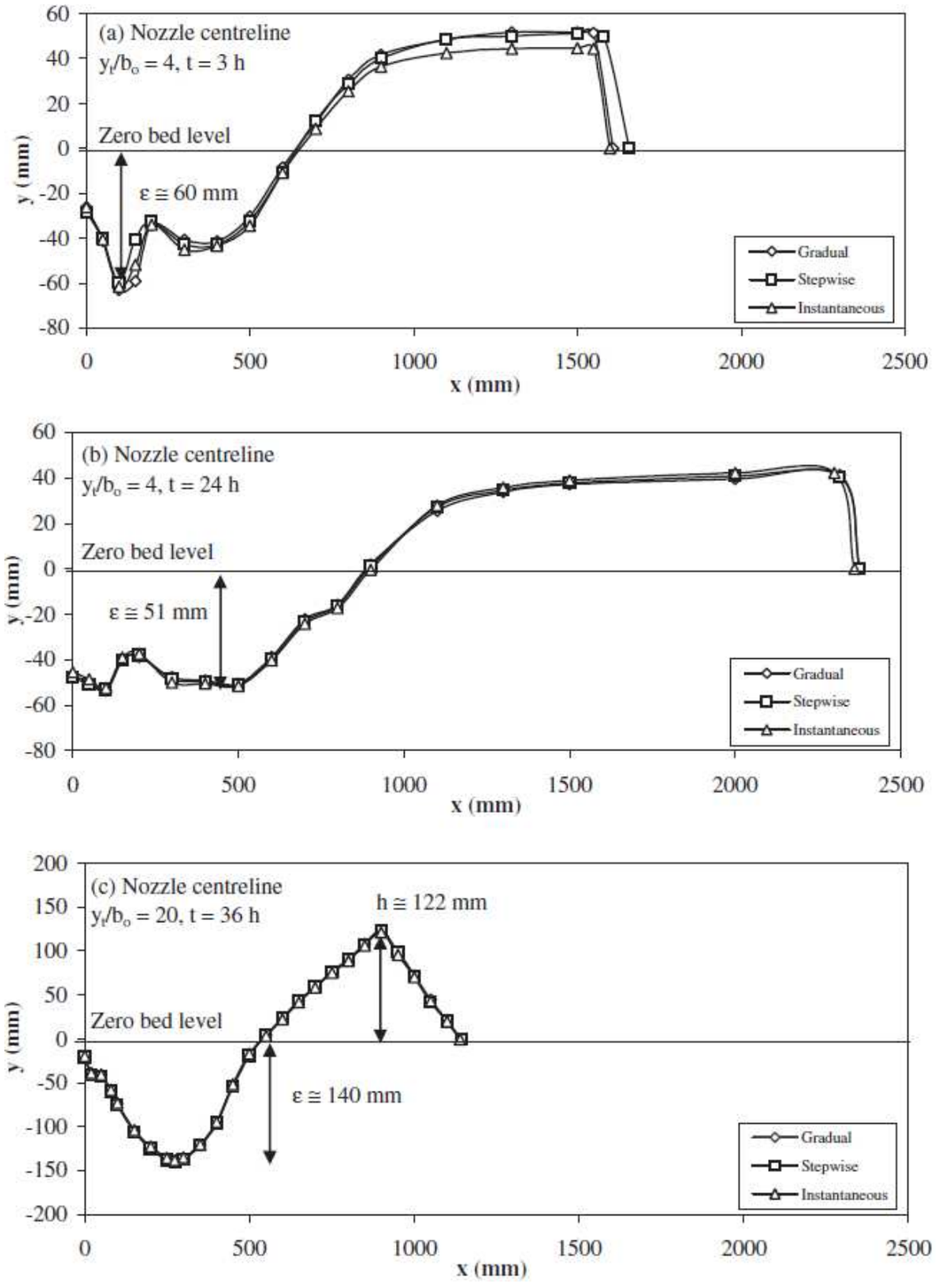

Figure 11. Effects of test startup conditions on the scour hole profiles (Deshpande et al. 2007, copyright permission of Taylor and Francis)

Fig. 10 shows the velocity-time history near the nozzle exit for three startup conditions at a low submergence ($H/b_o = 4$). Velocity data clearly indicate that there is no large scale scour upto about 150 s for stepwise and gradual change in flow. Velocity profile shows a significant dip in the mean velocity accompanied by large scale increase in turbulence after 150 s which indicates large scale scour. Further increase in valve opening increases velocity and large scale scour and causes higher turbulent intensities. For $t > 400$s, there is the presence of low frequency fluctuations. It was also found that a steady state velocity was attained after $t = 2000$ s in the case of stepwise startup condition and after $t = 600$ s in the case of gradual startup condition.

Fig. 11(a) shows the effect of the startup conditions on scour at $H/b_o = 4$ at 3h from the commencement of the flow. There are no significant differences in the profiles that can be attributed to startup conditions. However, the step wise and gradual startup conditions influence the mound to be slightly bigger and longer. It was observed that the digging phase continued for a longer time for these two startup conditions as compared to instantaneous condition. As a result, there has been more digging action and this is reflected in the profiles. This is an important aspect to note while comparing scour profiles with different startup conditions. Fig. 11(b) illustrates the profiles along the nozzle centerline for three startup conditions at 24h from the commencement of the test for $H/b_o = 4$. No significant differences can be found in the profiles and any minor differences that were noticed earlier have vanished. Figure 11(c) shows the scour profiles at the three startup conditions at $t = 36$ h at $H/b_o = 20$. Clearly the effects of test startup conditions are not evident at $t = 36$h. It was concluded that the effects of test startup conditions did not influence the long term scouring process.

9. Effect of channel width on local scour

Lim (1995) pointed out that the scour profile is not affected by the channel sidewalls when the expansion ratio is ten or greater. He also noted that the downstream channel would affect the lateral development of the scour hole if it becomes too narrow and restrict the normal diffusion of the three-dimensional jet. However, Faruque et al. (2006) have noted that scour hole dimensions are affected by the width of the downstream channel even for an expansion ratio (ER) as high as 14.5. They reported that the occurrence of the secondary ridges along the wall should be an effect of the jet expansion ratio. Faruque et al. (2006) and Sarathi et al. (2008) found that no secondary effects were observed for an ER of 41.4.

The effect of channel width on the extent of scour with varying tailwater conditions has been documented by Bey et al. (2008). They investigated the effect of jet exit velocity, tailwater depth and channel width concurrently on the scour characteristics. To this end, Bey et al. (2008) studied four groups of tests (denoted as A, B, C and D) using LDA and scour profile measurements to characterize the flow field. Tests were conducted at four widths ($w = 0.25\,W$, $0.5W$, $0.75\,W$ and W) and three different jet exit velocities ($U_o = 0.75$, 0.90 and 1.16 m/s). Here, W denotes a width of 0.4 m. In group A, for a given jet velocity and channel width, the submergence was varied in a stepwise fashion from a low tailwater ($y_t = 2b_o$) to a high tailwater condition ($y_t = 20b_o$). The tests in group B were commenced from a high submergence condition

http://dx.doi.org/10.5772/54909

(y_t = 20b_o) with a stepwise reduction towards low submergence. Group C tests were chosen such that the jet would continue to flip alternately between the bed and the free surface, and yet be close to the high submergence range at a given exit velocity. Group D tests were carried out at a fixed tailwater depth (y_t = 20b_o) for a period of 24 hours and velocity measurements are obtained at various time intervals. The results of varying channel width on bed scour profile variation are illustrated in Figs. 12 and 13.

Figure 12(a) and (b) shows the scour profiles for group C and group D for U_o = 1.16 m/s at various channel widths at t = 24 h. It can be observed from Fig. 12 that the scour profiles are dependent on channel width. The maximum scour depth decreases as the channel width increased from w= 0.25W to 0.75W. However, the maximum scour depth at w= 1.0 W is more than at w = 0.25W and 0.75W. From Fig. 12(b), it is observed that the maximum scour depth decreases with decreasing channel width. For all other conditions maintained constant, at higher submergence, it can be seen from the results that as the channel width increases, the maximum scour hole depth decreases, followed by an increase in maximum scour hole depth with further increase in width, whereas, at lower submergence, the scour hole depth decreases with decreasing channel width. The elongated mound and the formation of an intermediate hump in the scour hole near the nozzle (Fig. 12b) have been also observed in previous studies of Kells et al. (2001) and Deshpande et al. (2007).

Figure 13(a) and 13(b) shows the variation of maximum depth (ε) of scour at t = 24 h for test groups A and C, respectively. It can be noted that maximum depth of scour is a function of jet exit velocity and channel width. Available data from literature with comparable values of densimetric Froude number (F_o) are also shown in Fig. 13. It is observed from Fig. 13 that scour depth is different for the group A and C for any given channel width.

Sui et al. (2008) studied scour caused by 3D square jets interacting with non-cohesive sand beds to further understand the effects of channel width, tailwater conditions and jet exit velocity. The tailwater ratio was varied from 2 to 12 times the nozzle width, while the channel width was 31.6 and 41.4 times the nozzle width. Three different jet exit velocities were adopted and two different bed materials fine sand (d_{50}= 0.71 mm) and coarse sand (d_{50}= 2.30 mm) was used. Fig. 14 presents the variation of the different scour parameters with varying expansion ratio and tailwater ratio for both fine (Fig. 14a-c) and coarse sand (Fig. 14d-f). As shown in Fig. 14a, it can be noted that the maximum scour width increases with increasing ER and attains a maximum value at a tailwater ratio (TWR) = 4 for the tests with ER = 41.4. Increase of TWR results in a decrease of maximum scour width. For TWR > 3, length of scour hole (L_s) decreases with increasing ER. From Fig. 14b, it can be observed that maximum ridge width increases with increasing ER. It is also observed that the maximum length of scour hole is shorter for the higher ER for TWR > 3. Figs. 14d-f show the variation of the scour geometry parameters for the coarser sand at the two expansion ratios. Fig. 14d shows that the maximum width of scour is smaller for the higher expansion ratio for 3 ≤ TWR ≤ 4 and the maximum width of scour is higher for higher expansion ratio for TWR > 4.5. It is observed from Fig. 14d that the effect of ER on maximum scour width decreases with increasing sand grain size. Fig. 14e shows that there is no effect of ER on ridge width for coarse sand. Length of scour hole increases with decreasing ER (Fig. 14f). One can conclude the following from the study of Sui et al. (2008):

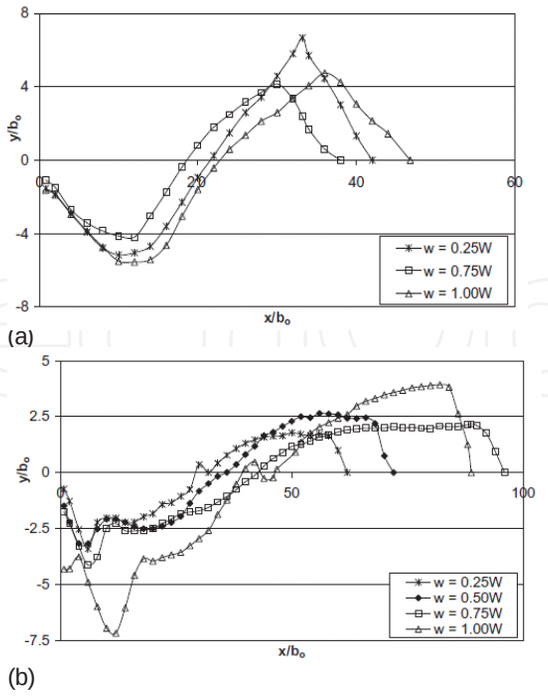

Figure 12. a) Scour profile variation with channel width with U_o = 1.16 m/s for group D, (b) Scour profile variation with channel width with U_o = 1.16 m/s for group C (Bey et al. 2008, copyright permission of Taylor and Francis

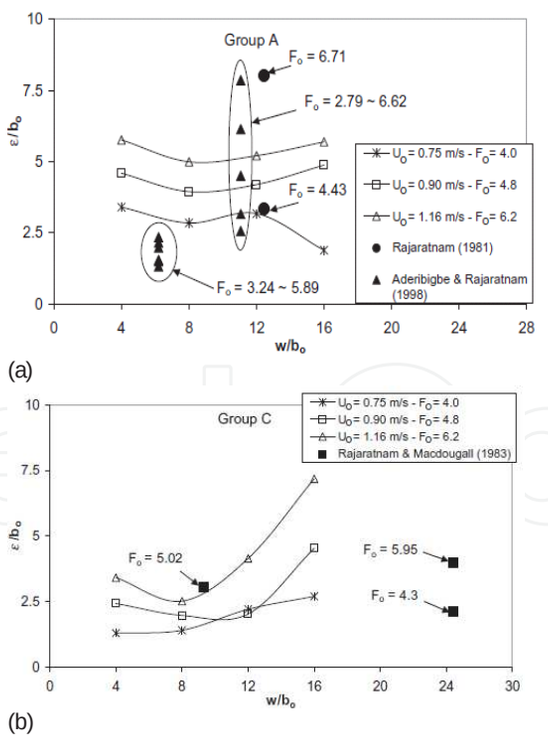

Figure 13. a) Plots of maximum scour depth with channel width for various velocities in group A, (b) Plots of maximum scour depth with channel width for various velocities in group C (Bey et al. 2008, copyright permission of Taylor and Francis)

i. For the fine sand and for TWR > 3, scour hole was wider but shorter in length at the higher expansion ratio. For the coarse sand, a similar trend was observed for TWR > 4.

ii. For the coarse sand and for 3 ≤ TWR ≤ 4, scour hole is strongly dependent on the tailwater ratio, especially at the lower expansion ratio.

iii. The effect of expansion ratio reduces as densimetric Froude number increases.

iv. The extent of difference for different scour parameter due to expansion ratio reduces with increasing TWR irrespective of the sand grain size.

v. Effect of ER reduces with increasing sand grain size.

vi. Results indicate that different expansion ratios create different scour profiles even for TWR ≥ 12.

vii. In an effort to provide useful, but a simplified scour prediction equation at asymptotic conditions, a relationship for the maximum scour depths has been proposed in terms of densimetric Froude number, tailwater ratio and expansion ratio.

viii. Proposed relationship predicted scour depths correctly for a wide range of test conditions.

10. Influence of densimetric Froude number on local scour

To better understand the scouring process, jets interacting with sand beds have been studied by many researchers and empirical relations involving densimetric Froude have been proposed to predict local scour. Rajaratnam and Berry (1977) studied the scour produced by circular wall jets and concluded that the main geometric characteristics of the scour hole are functions of the densimetric Froude number. Rajaratnam and Diebel (1981) concluded that the relative tailwater depth and width of the downstream channel only affect location of the maximum scour, whereas densimetric Froude number affects maximum scour depth. Ali and Lim (1986) indicated that the value of the critical tailwater condition increases with increasing densimetric Froude number and the effect of tailwater becomes insignificant when H/b_o is beyond 16. Chiew and Lim (1996) studied local scour by deeply submerged circular jets of both air and water and concluded that the densimetric Froude number was the characteristic parameter in describing the scour hole dimensions. Ade and Rajaratnam (1998) noted that the maximum depth of scour was larger at higher values of F_o. It was also noted that to attain an asymptotic state at higher values of F_o, a longer time was required. Faruque et al. (2004) concluded that the densimetric Froude number, tailwater depth and nozzle size-to-grain size ratio, all have an influence on the extent of scour caused by 3-D jets. They speculated about the dominance of each parameter at different flow conditions.

Sarathi et al. (2008) studied effect of the densimetric Froude number, tailwater depth and sediment grain size on scour caused by submerged square jets. Results of their study with respect to densimetric Froude number are presented in this section. Figures 15(a-c) show the

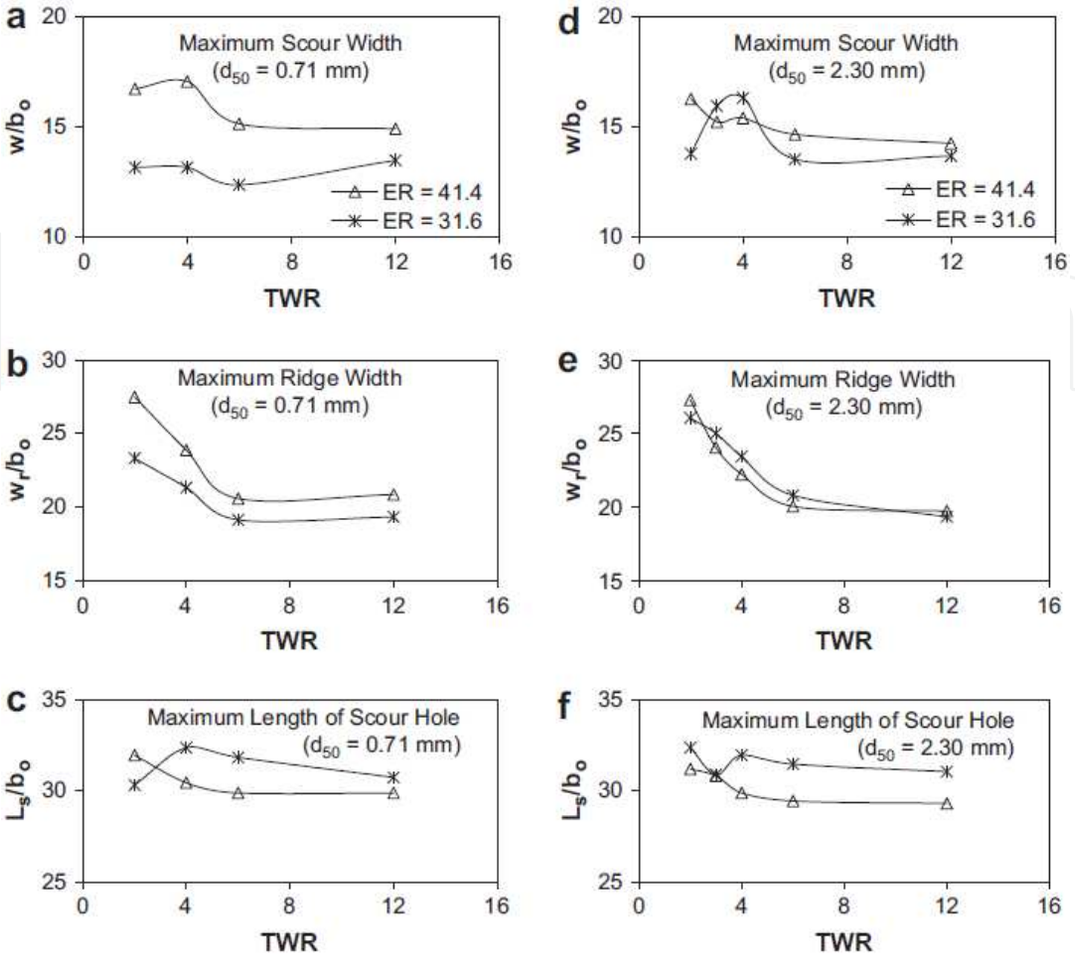

Figure 14. Variation of different scour parameters with respect to tailwater ratio (TWR) for F_o= 10, fine sand (d_{50}= 0.71 mm) and coarse sand (d_{50}= 2.30 mm) (Sui et al. 2008, copyright permission of Science Direct)

asymptotic scour profiles along the centerline of the nozzle for different F_o values. The asymptotic shape of the scour bed profiles for different F_o at H/b_o = 18 are shown in Fig. 15(a). It is observed that the maximum ridge height and its location, maximum scour depth and the distance of the maximum depth of scour hole from the nozzle (x_m) increases with increasing F_o. Figure 15(b) shows the scour profiles at three different values of F_o at lower tailwater conditions (H/b_o=2). The ridge crest is sharper at the lower value of F_o and at higher F_o the ridge is flat and directly related to the prevailing local velocity. Figure 15(c) shows the profiles at different F_o for H/b_o = 1. Ridge crests are flat and they are of constant height at different densimetric Froude numbers. It is clear that the size and shape of the ridge is clearly dependent on F_o and tailwater depth. Figure 15(d) shows the variation of the ridge height for different densimetric Froude numbers and tailwater depth. Ridge height is higher with higher densimetric Froude number. Ridge height increases with increasing tailwater depth for a given F_o however, beyond H/b_o = 6 for a given F_o, the ridge height attains a near constant value. Figure 16(a-c) shows the dependence of the normalized asymptotic scour parameters on F_o for a range of tailwater ratio. Figure 16(a) shows asymptotic maximum scour depth (ε_m) is higher for higher densimetric Froude number irrespective of the tailwater depths. Figure 16(b) and 16(c) show

http://dx.doi.org/10.5772/54909

similar trends of width of scour hole and length of scour hole. Scour hole dimensions are higher for higher densimetric Froude numbers. Finally, Sarathi et al. (2008) concluded that the role of grain size was completely absorbed by densimetric Froude number.

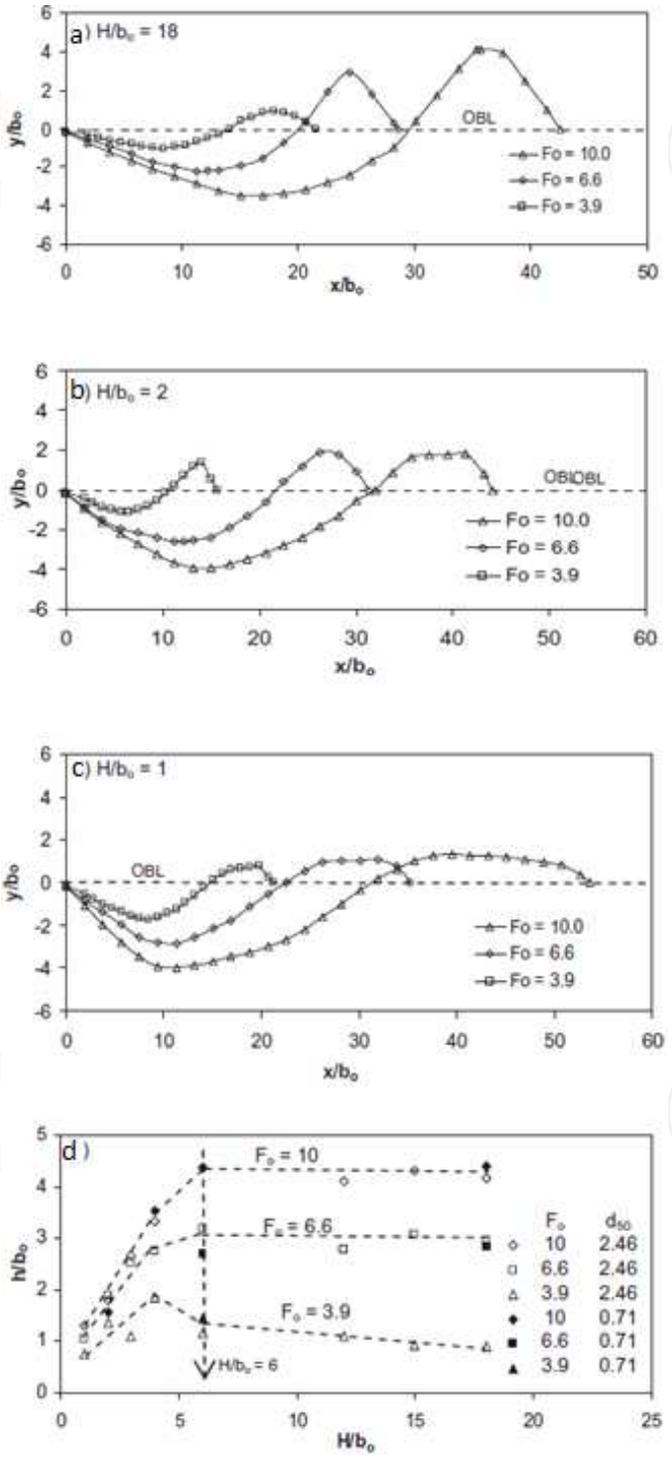

Figure 15. Scour geometry at asymptotic conditions at different densimetric Froude numbers (Sarathi et al. 2008, copyright permission of Taylor and Francis)

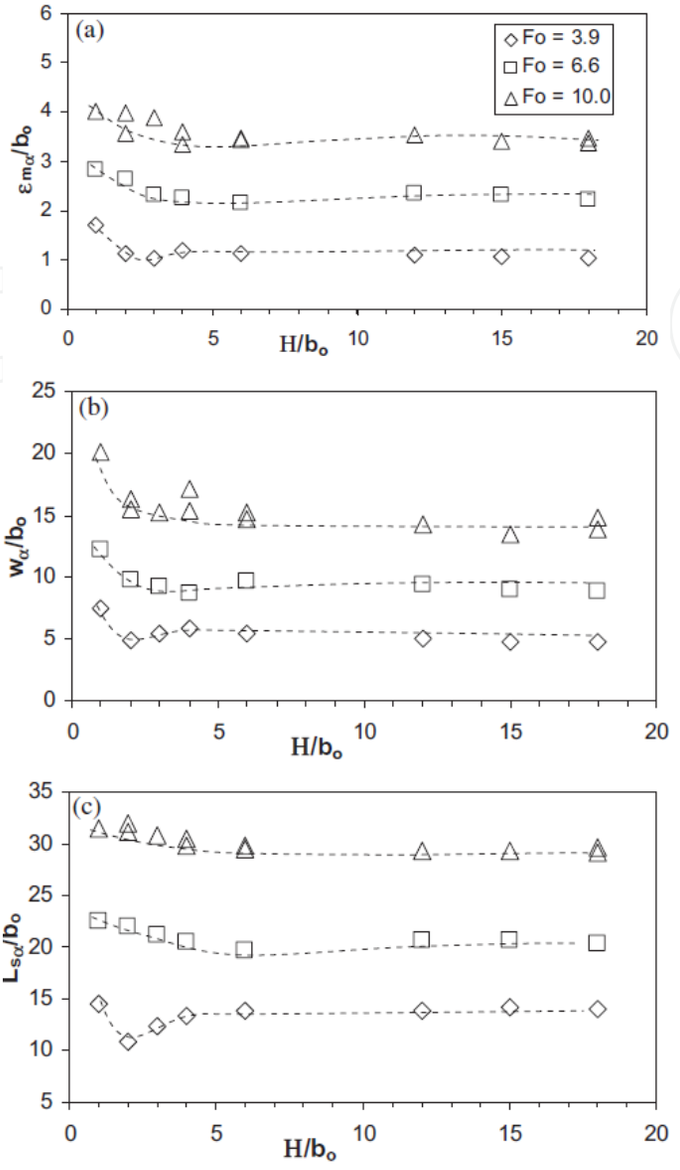

Figure 16. Variation of the asymptotic scour parameters with densimetric Froude number (Sarathi et al. 2008, copyright permission of Taylor and Francis)

11. Local scour under ice cover

Ice covers in rivers effect the resistance to flow, flow velocity and depth. Ice cover on top of the river with high sediment transport influences the development, size and shape of bedforms. This section reviews ice cover influences on the relationships between flow and local scour.

Ettema (2002) published an in-depth review on extent to which alluvial channels respond to ice-cover formation, presence, and breakup. An imposed ice cover results in an increased

composite resistance to the flow. Ice cover thickness affects only a comparatively narrow region near the upper level of flow in deep flows. On the other hand, in shallow flows, an ice cover chokes the flow, which decreases the velocity resulting in the bed shear stress to be less than the critical shear stress, and thereby decreases sediment transport. The studies also confirm that sediment-transport rate increases with decreasing water temperature. The location of the maximum velocity is dependent on the relative magnitudes of the channel bed and cover underside resistance coefficients (Gogus and Tatinclaux, 1981). The bed elevation in an ice covered stream must rise locally due to decrease in bulk velocity.

Asymptotic scour in the presence of smooth and rough ice cover was investigated by Sui et al (2009) and arrived at the following conclusions:

i. The variation of maximum scour depth with tailwater ratio under covered flow was different from that under open-water flow.

ii. Under open-water flow conditions, maximum scour depth decreased with increasing tailwater depth, and beyond a certain tailwater depth, the values tend to increase and attain constancy.

iii. Under covered flow, maximum scour depth increased with increasing tailwater depth, and beyond a certain tailwater depth, the values tend to decrease and attain constancy.

iv. Ice cover conditions do not influence maximum scour depth at large values of submerged conditions the.

v. Maximum scour depth in the fine sand bed under ice covered flow was always less than that noticed in the coarse bed material.

vi. Impact of ice cover on scour depth was also less obvious for finer sand.

vii. There was a negligible effect of ice cover on the scour parameters at lower densimetric Froude number.

viii. Scour width increased with increasing tailwater depth but decrease with increasing tailwater depth beyond a critical value and finally attained an asymptotic width in free surface and with fine sand bed.

ix. In the case of the coarse sand, scour length was larger under rough ice cover condition, but in the case of the fine sand, scour length was larger under open-flow condition.

x. Ridge height was not affected by type of bed material and with or without ice covered flow.

12. Numerical modeling of scour caused by jets

Numerical modeling is gaining momentum since experimental investigations are time consuming and expensive. Li and Cheng (1999) proposed a mathematical model based on

potential-flow theory for simulating the equilibrium scour hole underneath offshore pipelines. Karim and Ali (2000) tested effectiveness of a commercial software (FLUENT) to predict 2-D flow velocity distribution and the bed shear stress generated by a turbulent water jet impinging on rigid horizontal and scoured beds. Minimal and deeply submerged water jet simulations were carried out. The close agreement between selected various experimental and computed results were noted. The standard $k-\varepsilon$ and the RNG $k-\varepsilon$ models described the flow at the boundary better than the Reynolds stress model (RSM).

Neyshabouri et al. (2003) attempted to obtain numerical predictions of the scour hole geometry created by a free falling jet. The two-dimensional momentum equations, the continuity equation were solved using a $k-\varepsilon$ turbulence model. First, the turbulent flow due to a free falling jet was computed, then the distribution of the sand concentration was determined based on the convection-diffusion equation and the scoured bed was computed based on sediment continuity equation. The above-mentioned steps were repeated until the equilibrium scour hole was reached. Sediment transport calculations required specification of the sediment concentration near the bed at the start of simulation. Stochastic and deterministic expressions for sediment concentration near the bed proposed by van Rijn (1987) were used. The scour profiles obtained using stochastic expression was most realistic as compared to using of deterministic expression.

Adduce and Sciortino (2006) numerically and experimentally investigated local scour in clear water scour conditions downstream of a sill followed by a rigid apron. A mathematical one-dimensional model was developed which uses measured velocity fields (obtained using a ultrasonic Doppler velocimeter) to simulate the scour hole evolution. The dune profiles predicted by the model were similar to the measured profiles for large discharges, while when the discharges were smaller, the dunes predicted by the model were always longer than those measured.

Adduce and La Rocca (2006) studied different scour developments caused by a submerged jet, the surface wave jet and the oscillating jet developed downstream of a trapezoidal drop followed by a rigid apron. They have highlighted that as flow separation takes place at the edge of the rigid bed, reverse circulation motion along the longitudinal section develops near the bed downstream of the rigid bed itself. A stability analysis of the surface wave jet with both a flat and a scoured bed was performed by using modified Saint-Venant equations with correction terms accounting for the curvature of the streamlines. They concluded that the stability of the surface wave jet is weakened by the presence of the scoured bed.

Boroomand et al. (2007) mathematically modeled an offset jet entering a domain with sediment bed using ANSYS FLUENT with a two phase model in which water was primary phase and sediment bed was the secondary phase. In multiphase models, setting up of initial conditions is very important. These conditions include initial grid generation, initial phases and their properties and volume fractions of each phase. The model determines the interphase exchange coefficients, lifting force, virtual mass force, and interaction force between phases and solves the continuity and momentum equations for each phase. Scour profiles calculated by the model agreed fairly with the measurements. Also, the computed concentration profiles agreed fairly with measurements except near the bed zone.

http://dx.doi.org/10.5772/54909

Liu and Garcia (2008) studied turbulent wall jet scour in which bed evolution was modeled by solving the mass balance equation of the sediment. The free surface was modeled by the VOF method while the scour process was modeled by the moving mesh method. The modeling effort yielded a good agreement with measurements (velocity field, the maximum scour depths and local scour profile). Further research is needed to investigate the effect of the turbulence model for free surface waves (especially for near breaking and breaking waves) and to study the possibility of using an Eulerian approach for morphological modeling.

Abdelaziz et al. (2010) developed a bed load sediment transport module and integrated into FLOW-3D. This model was tested and validated by simulations for turbulent wall jet scour in an open channel flume. Effects of bed slope and material sliding were also taken into account. The hydrodynamic module was based on the solution of the three-dimensional Navier-Stokes equations, the continuity equation and $k-\varepsilon$ turbulence closure scheme. The rough logarithmic law of the wall equation was iterated in order to compute shear velocity u_*. The predicted local scour profile fit well with the experimental data, however the maximum scour depth was slightly under estimated and the slope downstream of the deposition dune was over estimated.

13. Scope for future research

The review of literature and our current understanding of scour by jets indicate that the following need to be considered in the future:

i. Extend studies to include cohesive soils.

ii. Extend studies to higher range of densimetric Froude number ($F_o > 10$).

iii. Non-uniform sand beds need to be studied to determine the effect of different gradations.

iv. To study the role of fluid structures with varying submergence, expansion ratio and nozzle size to grain size ratio.

v. Developing analytical equations for three-dimensional scour volume.

vi. To understand the effect of the removal of the mound at the asymptotic state, on scour depth, and 3-D scour hole development with time.

vii. To investigate separation, recirculation and eddies during digging and refilling phases at various submergence ratios.

viii. Obtain instantaneous velocity fields during scour hole development to enhance modeling efforts

ix. To study jet scour together with sediment transport by considering continuous sediment influx through the jet and in the ambient flow.

Author details

Ram Balachandar and H. Prashanth Reddy

Department of Civil and Environmental Engineering, University of Windsor, Canada

References

[1] Abdelaziz, S, Bui, M. D, & Rutschmann, P. Numerical simulation of scour development due to submerged horizontal jet", River Flow (2010). Dittrich, Koll, Aberle and Geisenhainer (eds), 978-3-93923-000-7, 2010.

[2] Adduce, C. La Rocca, M. ((2006). Local scouring due to turbulent water jets downstream of a trapezoidal drop: Laboratory experiments and stability analysis. Water Resour. Res. 42(2), W, 02405, 1-12.

[3] Adduce, C, & Sciortino, G. (2006). Scour due to a horizontal turbulent jet: Numerical and experimental investigation. J.Hydraulic Res. 44(5), 663-673.

[4] Ade, F, & Rajaratnam, N. (1998). Generalized study of erosion by circular horizontal turbulent jets, J. Hydraulic Res. 36(4), 613-635.

[5] Aderibigbe, O, & Rajaratnam, N. (1998). Effect of sediment gradation of scour by plane turbulent wall jets." J. Hydraul. Eng. 10.1061/(ASCE)0733-9429(1998)124:10(1034), 124 (10), 1034-1042.

[6] Aderibigbe, O, & Rajaratnam, N. (1996). Erosion of loose beds by submerged circular impinging vertical turbulent jets, J. Hydraulic Res, 34(1), 19-33.

[7] Ali, K. H. M, & Lim, S. Y. (1986). Local scour caused by submerged wall jets, Proc. Ins Civil Engineers. 81(2), 607-645.

[8] Ankamuthu, S, Balachandar, R, & Wood, H. (1999). Computational Steroscopy for Three-dimensional Scour Depth Measurement in Channels. Can. J. Civ. Eng., , 26, 698-712.

[9] Balachandar, R, & Kells, J. A. (1997). Local channel scour in uniformly graded sediments: The time-scale problem." Can. J. Civ. Eng. 10.1139/cjce-24-5-799, 24 (5), 799-807.

[10] Balachandar, R, & Kells, J. A. (1998). Instantaneous water surface and bed scour profiles using video image analysis." Can. J. Civ. Eng. 10.1139/cjce-25-4-662, 25 (4), 662-667.

[11] Balachandar, R, Kells, J. A, & Thiessen, R. J. (2000). The effect of tailwater depth on the dynamics of local scour." Can. J. Civ. Eng., 27 (1), 138-150.

[12] Bey, A, Faruque, M. A. A, & Balachandar, R. (2007). Two Dimensional Scour Hole Problem: Role of Fluid Structures". J. Hydraul. Engng. 133(4), 414-430.

[13] Bey, A, Faruque, M. A. A, & Balachandar, R. (2008). Effects of varying submergence and channel width on local scour by plane turbulent wall jets". J.Hydraul. Res. 46(6), 764-776.

[14] Boroomand, M, Neyshabouri, R, & Aghajanloo, S. , A. , S. K., ((2007). Numerical simulation of sediment transport and scouring by an offset jet", Can. J. Civ. Eng., , 34

[15] Breusers, H. N. C, & Raudkivi, A. J. (1991). Scouring, Hydraulic Structure Design Manual. A. A. Balkema, Rotterdam. The Netherlands.

[16] Chatterjee, S. S, Ghosh, S. N, & Chatterjee, M. (1994). Local scour due to submerged horizontal jet." J. Hydraul. Eng., 120 (8), 973-992.

[17] Chiew, Y. M, & Lim, S. Y. (1996). Local Scour by a Deeply Submerged Horizontal Circular Jet". J. Hydraul. Engng 122(9), 529-532.

[18] Day, R. A, Liriano, S, & White, R. W. (2001). Effect of tailwater depth and model scale on scour at culvert outlets, Proceedings of the Institution of Civil Engineers Water and Maritime Engineering, 148(3), 189-198.

[19] Deshpande, N. P, Balachandar, R, & Mazurek, K. A. (2007). Effects of submergence and test startup conditions on local scour by plane turbulent wall jets Journal of Hydraulic Research, 45 (3) (2007), , 370-387.

[20] Dey, S, & Sarkar, A. (2006a). Scour downstream of an apron due to submerged horizontal jets." J. Hydraul. Eng., 132(3), 246-257.

[21] Dey, S, & Sarkar, A. (2006b). Scour response of velocity and turbulence in submerged wall jets to abrupt change from smooth to rough beds and its application to scour downstream of an apron." J. Fluid Mech., , 556, 387-419.

[22] Ettema, R. (2002). Review of alluvial-channel responses to river ice." J. Cold Reg. Eng., 16(4), 191-217.

[23] Faruque, M. A. A, Sarathi, P, & Balachandar, R. (2006). Clear Water Local Scour by Submerged Three-Dimensional Wall Jets: Effect of Tailwater Depth," J. Hydraul. Engng. 132(6), 575-580.

[24] FaruqueMd. ((2004). Transient local scour by submerged three dimensional wall jets, effect of the tailwater depth. Msc thesis, University of Windsor.

[25] Ghodsian, M, Melville, B, & Tajkarimi, D. (2006). Local scour due to free overfall jet, Ins Civil Engineers, Water Management. 159(4), 253-260.

[26] Hoffmans, G. J. C. M. (1998). Jet scour in equilibrium phase", Journal of Hydraulic Engineering, , 124(4), 430-437.

[27] Hoffmans, G. J. C. M, & Pilarczyk, K. W. (1995). Local scour downstream of hydraulic structures", Journal ofHydraulic Engineering, , 121(4), 326-340.

[28] Hogg, A. J, Huppert, H. E, & Dade, W. B. (1997). Erosion by planar turbulent wall jets." J. Fluid Mech., , 338, 317-340.

[29] Hopfinger, E. J, Kurniawan, A, Graf, W. H, & Lemmin, U. (2004). Sediment erosion by Götler vortices: The scour problem." J. Fluid Mech., , 520, 327-342.

[30] Johnston, A. J. (1990). Scourhole Developments in Shallow Tailwater". J. Hydraul. Res., IJHR 28(3), 341-354.

[31] Karim, O. A, & Ali, K. H. M. (2000). Prediction of flow patterns in local scour holes caused by turbulent water jets. J. Hydraul. Res. , 38, 279-287.

[32] Kells, J. A, Balachandar, R, & Hagel, K. P. (2001). Effect of grain size on local channel scour below a sluice gate." Can. J. Civ. Eng. 10.1139/cjce-28-3-440, 28 (3), 440-451.

[33] Li, F, & Cheng, L. (1999). A numerical model for local scour under offshore pipelines J. Hydraul. Eng., 125 (4), , 400-406.

[34] Lim, S. Y. (1995). Scour below unsubmerged full flowing culvert outlets. Proc. Ins Civil Engineers, , 112, 136-149.

[35] Liu, X, & Garcia, M. H. (2008). Three-dimensional numerical model with free water surface and mesh deformation for local sediment scour. Journal Waterway, Harbour, Coastal and Ocean Engineering, ASCE 134 (4), 203-217.

[36] Mazurek, K. A, & Rajaratnam, N. (2002). Erosion of a polystyrene bed by obliquely impinging circular turbulent air jets, J. Hydraulic Res. 40(6), 709-716.

[37] Mehraein, M, & Ghodsian, M. and Salehi Neyshaboury, S. A.A ((2010). Local scour due to an upwards inclined circular wall jet, Proc. Ins Civil Engineers, , 164, 111-122.

[38] Melville, B. W, & Chiew, Y-M. (1999). Time scale for local scour at bridge piers. ASCE Journal of Hydraulic Engineering, , 125(1), 59-65.

[39] Meulen, V, Vinje, T, & Three-dimensional, J. , J. local scour in noncohesive sediments", Proc., 161th International Association for Hydraulic Research (IAHR)-Congr., San Paulo, Brazil, , 263-270.

[40] Mih, W. C, & Kabir, J. (1983). Impingement of Water Jets on Non uniform S treambed, J. Hydraulic Eng. 109 (4), 536-548.

[41] Mohamed, M. S, & Mccorquodale, J. A. (1992). Short-term local scour", Journal of Hydraulic Research, , 30(5), 685-699.

[42] Neyshabouri, S. A. A., Ferreira Da Silva, A. M. and Barron, R. (2003). Numerical Simulation of Scour by a Free Falling Jet. J. Hydraul. Res., , 41(5), 533-539.

[43] Neyshabouri, S. A. A, & Barron, R. Ferreira da Silva, A.M. ((2001). Numerical Simulation of Scour by a Wall Jet". Water Engng Res. 2(4), 179-185.

[44] Pagliara, S, Hager, W. H, & Minor, H. E. ((2006). Hydraulics of plane plunge pool scour. J. Hydr. Engng. 132(5), 450-461.

[45] Rajaratnam, N. (1981). Erosion by plane turbulent jets, J. Hydraulic Res. 19(4), 339-358.

[46] Rajaratnam, N, & Berry, B. (1977). Erosion by circular turbulent wall jets, J. Hydraulic Res. 15(3), 277-289.

[47] Rajaratnam, N, & Mazurek, K. A. (2003). Erosion of sand by circular impinging water jets with small tailwater, J. Hydraulic Eng. 129(3), 225-229.

[48] Rajaratnam, N, Aderibigbe, O, & Pochylko, D. (1995). Erosion of sand beds by oblique plane water jets." Proc. Inst. Civ. Eng., Waters. Maritime Energ., 112(1), 31-38.

[49] Rajaratnam, N, & Diebel, M. (1981). Erosion below Culvert-Like Structure". Proceeding of the 5th Canadian Hydrotechnical Conference, 26-27 May, CSCE, , 469-484.

[50] Rajaratnam, N, & Macdougall, R. K. (1983). Erosion by Plane Wall Jets with Minimum Tailwater". J. Hydrual. Engng., 109(7), 1061-1064.

[51] Sarathi, P, Faruque, M. A. A, & Balachandar, R. (2008). Influence of tailwater depth, sediment size and densimetric Froude number on scour by submerged square wall jets, J. Hydraulic Res. 46(2), 158-175.

[52] Sui, J, Faruque, M. A. A, & Balachandar, R. (2009). Local scour caused by submerged square jets under model ice cover, J. Hydraulic Eng., 135(4), 316-319.

[53] Sui, J, Faruque, M. A. A, & Balachandar, R. (2008). Influence of channel width and tailwater depth on local scour caused by square jets, J. Hydro-environment Res, 2(1), 39-45.

[54] Van Rijn ((1987). Mathematical Modeling of Morphological Processes in the Case of Suspended sediment transport. PhD. Dissertation, Delft University of Technology, The Netherlands.

[55] Wu, S, & Rajaratnam, N. (1995). Free jumps, submerged jumps, and wall jets." J. Hydraul. Res., 33(2), 197-212.

IntechOpen